Highway tunnel performance during the 1999 Duzce earthquake

Comportement de tunnels autoroutiers pendant le tremblement de terre de Duzce en 1999

T.D.O'Rourke & S.H.Goh – *Cornell University, Ithaca, New York, USA*
C.O.Menkiti – *Geotechnical Consulting Group, London, UK*
R.J.Mair – *University of Cambridge, Cambridge, UK*

ABSTRACT: This paper describes the effects of the M_w 7.2 1999 Duzce earthquake on 18-m-diameter highway tunnels near Bolu, Turkey, which were under construction. It provides a first time opportunity to evaluate the earthquake performance of tunnels in a variety of ground and support conditions in response to a near-source severe earthquake. Information about the tunneling conditions are summarized, including the geotechnical properties of the rock and soil units and general characteristics of the tunnel support system. The results of geotechnical instrumentation are presented to show that permanent increases in bending moment and compressive hoop stress, equivalent to about 17% of the overburden, were induced by ground shaking. Analyses were performed using measured strong ground motions for a damaged cross-section in fault gouge clay and the results are shown to agree favorably with observed performance.

RÉSUMÉ: Cet article décrit les conséquences du tremblement de terre de Duzce en 1999, de magnitude 7.2, sur les tunnels autoroutiers de 18m de diamètre situés près de Bolu en Turquie, à l'époque en phase de construction. Cet évènement a fourni la première occasion d'évaluer le comportement d'un tunnel vis-à-vis d'un tremblement de terre proche, avec des conditions de terrain et de support variées. Les informations relatives au creusement des tunnels sont résumées, notamment les propriétés géotechniques des différentes formations rocheuses et de sol, ainsi que les caractéristiques générales du système de support des tunnels. Les résultats découlant de l'instrumentation géotechnique sont présentés et montrent qu'une augmentation permanente du moment de flexion et de la contrainte de compression circulaire, équivalente à environ 17% de la surcharge, a été causée par le mouvement de tremblement du sol. A partir des forts mouvements de sol mesurés, des analyses ont été effectuées sur une section endommagée située dans une zone argileuse résultant de mouvements de faille, et il est montré que les résultats s'accordent favorablement avec le comportement observé.

1 INTRODUCTION

The twin highway tunnels, each 18 m in excavated diameter and 3.6 km in length, are located on the Gumosova-Gerede portion of the Northern Anatolian Motorway. Tunneling was performed according to NATM principles, with shotcrete, rock bolts, and light steel sets. The epicenter of the M_w 7.2 earthquake was located about 20 km from the western portals of the tunnels. The surface rupture of the causative fault was within 3 km of these portals. Observations show that the tunnels performed well, especially in the light of their close proximity to the seismic source. Some of the temporary shotcrete-supported sections, however, were heavily loaded by the earthquake such that collapses occurred at locations with the worst ground conditions and severe deformations were observed at other locations in clay fault gouge.

This paper provides information about the tunneling conditions, including the geotechnical properties of the rock and soil units, and general characteristics of the tunnel support system. The earthquake performance is described with reference to the support systems and ground conditions at various locations along the tunnels. The results of field instrumentation, which show significant increases in permanent hoop stress and bending moments after the earthquake, are presented. The analytical results of models that account for the seismic response to measured ground motions are summarized and compared with observed behavior.

2 TUNNELLING CONDITIONS

2.1 *Ground conditions*

The tunnels are being bored through highly tectonised and faulted sequences of rocks, including flysch, shale, sandstone, mudstone, marble, granite, and amphibolite. Ground cover to the tunnel centerline is 270m maximum, but typically 130m. The ground consistency varies from competent rock to continuous zones of pure fault gouge clay. Ground water level above the tunnel axis is 45 - 85% of the overburden cover.

In 1998/9, a detailed characterization of the ground ahead of the tunnel faces was implemented via a pilot tunnel test program. The identified geotechnical units and their mechanical properties are described in Tables 1 and 2.

Table 1. Geotechnical properties and ground conditions

Unit	Consistency	PI[1] (%)	CP[2] & Mineralogy
High PI flychoid clay	stiff, highly plastic, heavily slicken-sided, clay matrix with occasional rock fragments	55	35%-50%, smectite with traces of kaolin
Blocky flyschoid clay	medium plastic, silty clay matrix with gravel, cobbles & boulder sized inclusions	25	30%-50%, smectite with traces of kaolin
Area 3 fault gouge clay (ch 64140-64200)	highly plastic, heavily slicken-sided, stiff clay gouge	55	30%-60%
AS/EL fault gouge clays (ch 62840-62905)	very heavily slicken-sided, highly plastic, stiff to hard clay fault gouge.	40-60	20%-50%, smectite
Metasediments	gravel, cobbles and boulder sized shear bodies in soil matrix. Soil matrix is 20%-60% by volume	10-15	5% to 25%, illite (58%) & smectite (23%) predominant
Crushed MCB[3]	crushed, weathered, highly sheared, clayey, very weak rock with slicken-sided, sandy silty clay fault gouge matrix.	15	0%-20%
Sound MCB[3]	Fractured but competent rock with UCS[4] of 6-12 MPa.	NA[5]	NA[5]

1 Plasticity index 2 Clay percentage by weight (i.e. finer than 0.002mm)
3 Metacystalline basement rock 4 Unconfined compression strength
5 Not applicable

2.2 *Construction details*

These mixed ground conditions have made tunneling difficult. Excavation was performed according to NATM principles, with shotcrete, rock bolts, and light steel ribs as the primary support and a cast-in-situ concrete inner lining. Figure 1 shows a typical

Table 2. Measured strength and stiffness parameters

Unit	Peak		Residual		G_o/σ'_v [7]
	ϕ' [6]	c' [6] (kPa)	ϕ' [6]	c' [6] (kPa)	
High PI[5] flysch clay	15°-17°	100	9°-12°	50	500[1]
Blocky flysch clay	20°-25°	100	13°-17°	50	650[1]
Area 3 FG[3] clay	13°-16°	100	9°-12°	50	700[1]
AS/EL FG[3] clay	18°-24°	100	6°-12°	50	NA[4]
Metasediments	25°-30°	50	20°-25°	25	825[1]
Crushed MCB	20°-25°	50	15°-20°	25	950[1]
Sound MCB[2]	55°	1500	NA[4]	NA[4]	High

1 From high quality pressuremeter tests 2 Metacrystalline basement rock
3 Fault gouge 4 Not available 5 Plasticity index
6 ϕ', c' = effective stress friction angle and cohesion, respectively
7 G_o/σ'_v = ratio of max shear modulus to initial vertical effective stress

cross-section. The primary lining supports the immediate ground loads providing a stable environment in which the inner lining is installed to give the necessary long-term safety margin. For poor ground new designs were developed in which the primary support is augmented with an additional 60 - 80cm cast-in-situ concrete layer to provide stronger support close to the face, before the inner lining is cast. Mining commenced from both portals in 1993/4, progressing towards the center using conventional excavators (with limited lengths of drilling and blasting in very strong ground). Spoil is disposed using mechanical loaders and dumpers. Excavation is in variable round lengths, typically 1.1m. Full ring closure is achieved 1.3 - 2.5 tunnel diameters behind the face in poor ground and up to 5.5 diameters in better ground.

3 EARTHQUAKE PERFORMANCE

Inspection of the tunnels was carried out after the Duzce earthquake. The following damage patterns were noted.

3.1 *Completed main tunnel sections (primary and inner linings installed before the earthquake)*

The 2475m of completed tunnels performed remarkably well given the closeness of the seismic source. Only slight damage of the inner lining occurred as openings of the construction joints (1 - 5mm wide) between adjacent 13.5m long lining blocks. These joint openings did not affect the closed-ring load bearing function of the lining or compromise the water tightness functionality. Water tightness was achieved using a flexible membrane composed of PVC and geotextile felt. Its compliant nature was critical to successful earthquake performance. In segmental linings, for example, careful joint design would have been necessary to ensure similar performance. In addition to the joint openings, non-structural hairline cracks were observed in the crown area and at niche box-out corners.

3.2 *Shotcrete supported tunnel sections*

A wide range of damage severity, mainly dependent on the ground conditions, was observed in tunnel sections which were still under construction and only supported by the shotcrete lining. These are listed below for progressively worsening ground.

1. No damage was observed in a 5.8m diameter passenger cross-adit tunnel in Metasediments with 10% clay matrix, supported by 30cm thick shotcrete lining with a 28 day characteristic cube strength, f_{cu}, of 30MPa.
2. Slight-moderate damage was noted in the 16.5m diameter main tunnels within weaker Metasediments (30%-60% clay matrix) supported by a 45cm shotcrete lining of f_{cu} = 20MPa. Slabbing and spalling of shotcrete, and continuous longitudinal cracking along the potentially weak top heading–bench joint were observed.
3. Heavy to severe damage was observed in 5m diameter bench pilot tunnels within the AS/ EL fault gouge clay supported by 30cm thick shotcrete (f_{cu} = 30MPa) and HEB 100 steel ribs sets at 1.1m longitudinal spacing. (The HEB 100 is a 100mm x 100mm steel "T" section with a flange thickness of 10mm and a web thickness of 5.5mm.) Damage to the bench pilot tunnels comprised slabbing and spalling of shotcrete at crown and shoulder locations, compression crushing of shotcrete associated with buckling of HEB 100 steel ribs at shoulder and knee locations. At the shoulders in particular, the buckled configuration indicated shortening of steel ribs by 0.3m-0.4m such that at times the steel ribs were completely severed. Invert failure was inferred from bottom uplift of 0.5m-1.0m. The bench pilot tunnels were driven in parallel at a center-to-center separation of 18.5m, with one tunnel leading the other. Only slight damage was observed in portions of these tunnels in the better ground (Metasediments) leading to the main fault gouge clay where heavy damage occurred. More pronounced damage occurred in the lead tunnel, which was more heavily loaded prior to the earthquake. Strikingly, severe damage was strictly limited to the zone where the two tunnels "overlap" and are within the fault gouge clay. In the same clay, no damage occurred in the lead portion of the first tunnel.
4. Severe damage in the form of complete collapse of two parallel 16.5m diameter main tunnels occurred during the earthquake. The tunnels were excavated in the Area 3 main fault gouge clay, at a center-to-center separation of 54m and supported by 45cm-75cm of shotcrete (f_{cu} = 20/30 MPa). Large deformations necessitating re-profiling works had occurred in this area before the earthquake. During the earthquake itself, the right tube lining was breached with inrush of clayey material and complete blockage of the tunnel so that miners had to escape through a cross-adit and via the left tube. At this time the left tube was collapsing with falling blocks of shotcrete and clay. Within 1-2 hours of the main shock, the left tube too had become blocked by clay debris. The collapse in the right tube propagated upwards through 50m of cover to cause a 5m diameter sinkhole and concentric ground cracks at the surface during the earthquake. Progressive failure occurred, confirmed by the generation of another 8m diameter sink hole over the left tube, through 122m of cover, some 4.5 months after the earthquake. Drilling investigations completed 7 months after the earthquake indicate that about 360m of tunnel had experienced collapses in the right tube and about 170m in the left tube.

3.3 *Invert performance*

Moderate damage occurred as cracking of the deep monolithic concrete invert over about 700m of tunnels. Longitudinal tensile-type cracks (running close to the centerline) and shear-type cracks (running towards the invert sides) were observed. Crack widths were 0.5 - 5cm, depending on ground conditions, invert thickness and reinforcement levels. In comparison, the shotcrete arch invert performed better having experienced no visible earthquake damage.

4 INSTRUMENTATION RESULTS

Pre- and post-earthquake measurements were available at 5 different sections in the inner lining within clayey metasediments (depth 242-260m). Figure 2 shows the typical configuration with pressure cells and embedded strain gauges at various points around the inner lining. At each point, two strain gauges were installed to distinguish hoop stress and bending components. The lining hoop stress changes at the crown of Block 54 are also shown, as typical results. Stress changes are given relative to a point about 2.5 months before the earthquake. Data from the strain gauges are based on measured concrete Young's modulus. Significant permanent compression hoop stress increases were measured immediately following the earthquake, with a sagging mode of bending. Figure 3 shows the average hoop stress changes around the lining. Peak values of up to 10 MPa (equivalent to about 17% of the overburden) are induced at the crown and feet of the arch lining, representing a significant proportion of the strength reserve.

While it is widely appreciated that landslides and fault rupture can lead to high locked-in lining loads, it is not often understood that such loads can also be generated by ground shaking with the following mechanisms.

- Large cyclic shear stresses overload the ground annulus around the tunnel, creating a wider plastic zone and accumulating permanent lining strains and loads. Typically, this annulus is weakened apriori by construction induced deformations. Numerical studies indicate that permanent loads by this mechanism could be a large percentage of the peak dynamic loads.

- Cyclic stresses can generate pore pressures and thus permanent lining loads during the ensuing consolidation.
- In rocky ground, shaking may disrupt the pre-earthquake load arch around the tunnel such that a larger cone of loose ground is made to bear upon the lining.

5 ANALYTICAL RESULTS

The response of different tunnel linings in a variety of ground conditions, including both the absence and presence of damage, provides an opportunity to use the as-built records and post-earthquake observations at the Bolu Tunnels for calibrating and/or validating analytical models of tunnel response to earthquake excitation. Simplified models have been proposed by Penzien and Wu (1998) and adopted in FHWA guidelines (2000) for evaluating the seismic response of circular tunnels. As described previously, heavy to severe damage was observed in 5-m-diameter bench pilot tunnels (BPTs) in fault gouge. These tunnels were to be filled with lean concrete to provide a stable reaction base for the tunnel arch after subsequent enlargement of the underground opening.

Figure 4 shows a cross-section of the 5-m-diameter BPT and a schematic of circular tunnel deformation caused by vertically propagating shear waves. This type of shear deformation is assumed in the Penzien and Wu (1998) model that permits the calculation of both the earthquake-induced maximum thrust, T, and moment, M, as :

$$T = G_m D K \gamma_{smax} \quad (1)$$

$$M = (1/2)\, G_m D^2 K \gamma_{smax} \quad (2)$$

in which G_m is the effective shear modulus of the geologic medium, D is tunnel diameter, γ_{smax} is the maximum free field shear strain at tunnel level and $K = (1 - \nu_m)(F + 3 - \nu_m)^{-1}$ in which ν_m is Poisson's ratio of the geologic medium and F is the ratio of the shear stiffness of the geologic medium to that of the lining.

Analyses were performed with SHAKE91 (Idriss and Sun, 1992) using free-field strong motion recordings at ground surface in Bolu, approximately 12.5 km east of the tunnels. Figure 5 shows the corrected time records for acceleration and velocity in the east-west (E-W) direction. The E-W motion, which affects the transverse tunnel cross-section, was reduced by 30% to account for strong motion attenuation with depth in accordance with empirical data collected from deep vertical arrays at several sites in Japan and the US. The scaled input motion was introduced at the base of the gray sandstone and siltstone, treating the quartzitic rock as a rigid base.

The soil and rock strata and corresponding shear wave velocity, v_s, and maximum shear modulus, G_{max}, assumed for each stratum are shown in Figure 6 together with the maximum shear strain profile resulting from the SHAKE91 analyses. The actual G_{max} for each rock and soil type was estimated by means of a careful interpretation of pressuremeter test results in the rock/soil of interest for loading and unloading loops at small strain (0.002 to 0.01%) levels. Damping factor and G/G_{max} vs γ_s relationships for the clayey fault gouge were taken from Vucetic and Dobry (1991) for overconsolidated clay with a plasticity index of 50, and similar relationships for the remaining aranaceous rock strata were modeled after data published by Shibuya, et al. (1992) for cemented sand. Upper and lower bound estimates of v_s and G_{max} pertaining to fault gouge undisturbed and disturbed by tunneling resulted in maximum shear strains at the tunnel level of 0.14 and 0.18%, as shown in the figure.

Using the analytical shear strains in the Penzien and Wu equations above resulted in dynamic stresses that were combined with static stresses in the lining. The static stresses were estimated at approximately 40 to 50% of the overburden pressure on the basis of measurements at three instrumented sections in similar ground, convergence measurements at the BPTs, and numerical simulations. The earthquake-induced compressive

Table 3. Summary of Analytical Stresses and Crushing Strength of Linings for Bench Pilot Tunnels (BPTs).

Tunnel	Range of Analytical Strains	Maximum[1] Compressive Stress Due to Earthquake and Static Loading, MPa	Out Fiber[2] Crushing Strength of Shotcrete, MPa
Left BPT	0.14 - 0.18%	21.7 - 25.4	26.0
Right BPT	0.14 - 0.18%	17.0 - 19.1	17.5

1 Calculated using shotcrete stiffness estimated at time of earthquake
2 Estimated from shotcrete age at time of earthquake and measured in situ strength development

stresses in the lining were approximately equal to the existing static stresses.

Comparison of the analytical stresses due to static and earthquake loading with the crushing strength of the lining in Table 3 shows that the lining was loaded to and beyond failure of the shotcrete. The results compare favorably with the observed damage because compression crushing and rib buckling were observed after the earthquake. Moderate to severe damage was observed without full collapse. The analytical results are consistent with the post-earthquake observations in that the simplified model indicates that the lining should be overloaded but not to the extent of collapse or closure.

6 CONCLUDING REMARKS

Observations and analyses of the effects of the Mw=7.2 1999 Duzce earthquake on highway tunnels in Turkey are presented, which constitute a first time opportunity to evaluate tunnel earthquake performance to severe near-source ground motions. The tunnels were being constructed in a highly deformed and faulted sequence of rocks.

It was observed that completed sections of tunnels, where the primary and inner lining had been installed before the earthquake, performed remarkably well experiencing only slight damage. For uncompleted sections of tunnel, supported only by shotcrete, a wide range of damage was observed primarily dependent on the ground conditions. Tunnel performance ranged from no damage to severe deformations in poor ground, with collapse in zones of highly plastic, heavily slicken-sided fault gouge clay. Moderate cracking damage was observed in unreinforced or lightly reinforced deep monolithic concrete inverts in poor ground.

The results of geotechnical instrumentation show that permanent increases in bending moment and compressive hoop stress equivalent to about 17% of the overburden were induced by ground shaking.

Analytical results derived from simplified models of circular tunnel lining interaction with vertically propagating shear waves compare favorably with tunnel lining damage observed in the field. The Bolu Tunnels provide a valuable case history, useful for calibrating and/or validating a variety of analytical models for seismic tunnel response. Preliminary comparisons of observed damage with models of tunnel distortion by shear waves (e.g. Penzien and Wu, 1998) suggest that such simplified models provide a suitable basis for approximating tunnel performance and identifying potentially vulnerable conditions.

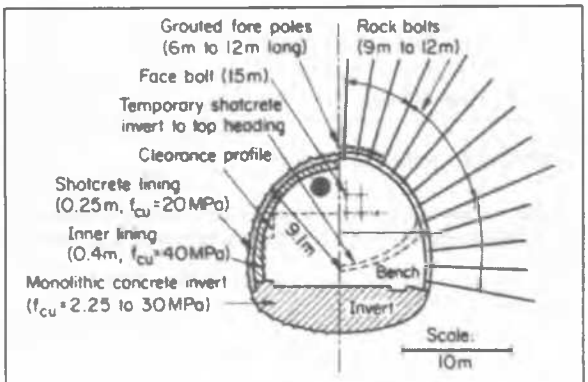

Figure 1. Typical Tunnel Cross-Section

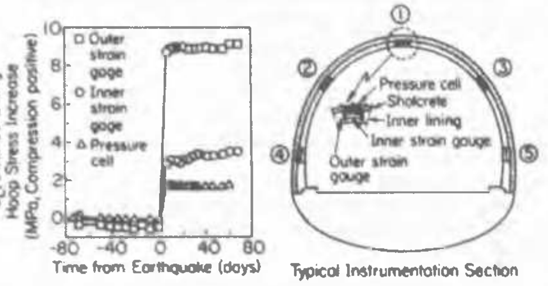

Figure 2. Hoop Stress and Pressure Cell Measurements Before and After the Earthquake

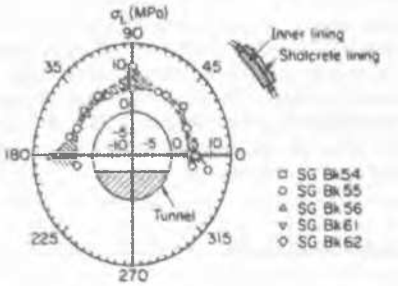

Figure 3. Average Increase in Hoop Stress After the Earthquake

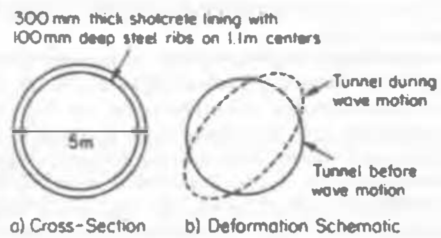

Figure 4. BPT Cross-Section and Seismic Distortion

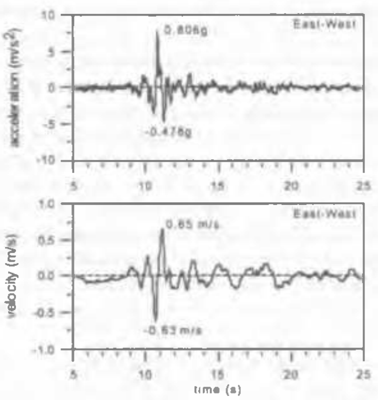

Figure 5. Strong Motion Time Records

7 ACKNOWLEDGEMENTS

The authors acknowledge the cooperation of KGM, Yuksel-Rendel JV, Astaldi-Bayindir JV, Lombardi Engineering Ltd. and Geoconsult.

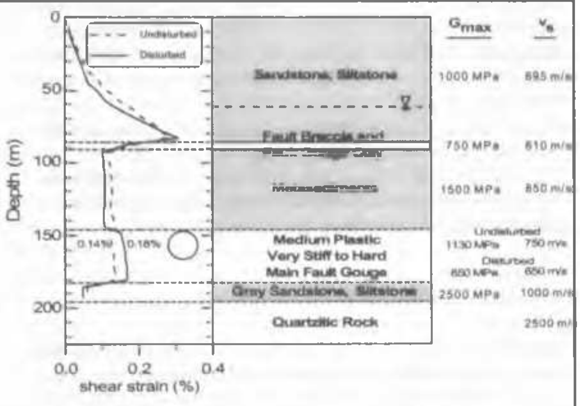

Figure 6. Shear Strains from One-Dimensional Modeling with Geologic Profile and Relevant Material Properties

REFERENCES

Federal Highway Administration (FHWA). 2000. *Seismic Retrofitting Manual for Highway Structures, Part II*. Prepared by Multidisciplinary Center for Earthquake Engineering Research, Buffalo, NY, in press.

Idriss, I.M., and Sun, J.I. 1992. *User's Manual for SHAKE91*. University of California at Davis.

Penzien, J., and Wu, C.L. 1998. Stresses in Linings of Bored Tunnels. *Earthquake Engineering and Structural Dynamics* 27 : 283-300.

Shibuya, S., Tatsuoka, S., Teachavorasinskun, S., Kong, X.J., Abe, F., Kim, Y-S., and Park, C-S. 1992. Elastic Deformation Properties of Geomaterials. *Soils and Foundations* 32(3) : 26-46.

Vucetic, M., and Dobry, R. 1991. Effect of Soil Plasticity on Cyclic Response. *Journal of Geotechnical Engineering* 117(1) : 89-107. ASCE.